

Characteristics of boiling heat transfer on hydrophilic surface with SiO₂ coating

A. S. Surtaev^{1,2*}, V. S. Serdyukov^{1,2}, A. N. Pavlenko¹, D. V. Kozlov^{2,3}, D. S. Selishchev^{2,3}

¹ Kutateladze Institute of Thermophysics, Siberian Branch of Russian Academy of Science, Novosibirsk, 630090, Russia; ² Novosibirsk State University, Novosibirsk, 630090, Russia;

³ Boreskov Institute of Catalysis, Siberian Branch of Russian Academy of Science, Novosibirsk, 630090, Russia

Received May 17, 2018, Accepted June 26, 2018

The paper presents the results of an experimental study of the effect of wetting properties on the local and integral characteristics of heat transfer at water boiling on the saturation line under atmospheric pressure. To control the wetting characteristics, the nanocoatings of SiO₂ were synthesized on the sapphire substrate surface using various chemical methods including dip coating and spin coating. New experimental data on dynamics of vapor bubble growth and detachment, evolution of microlayer and dry spot regions, nucleation site density and bubble emission frequency, heat transfer, etc., were obtained using the high-speed imaging techniques, including infrared thermography and video recording from the bottom side of transparent heater. The analysis of experimental data on the local and integral characteristics of the boiling process made it possible to determine the mechanisms of the influence of deposited hydrophilic coatings on the heat transfer intensity.

Keywords: Boiling, Hydrophilic coating, IR thermography, Heat transfer, Bubble dynamics

INTRODUCTION

It is well-known that the properties of heat exchange surfaces, especially wettability, significantly affect the dynamics of phase transition at boiling and condensation. Thus, for instance, the use of hydrophobic coatings allows to significantly increase the heat transfer coefficient at vapor condensation due to implementation of the dropwise condensation mode [1, 2]. The wetting properties also have a significant effect on the bubble dynamics, heat transfer and critical heat fluxes (CHF) at liquid boiling [1, 3-11]. For example, a theoretical expression for describing the effect of the contact angle on the CHF at liquid boiling is obtained by Kandlikar [5] based on the balance of forces acting on the individual bubble. Here, it is worth noting that this pioneering work is often cited when analyzing data on the crisis phenomena at boiling of nanofluids. This relates to the fact that when nanofluids (i.e. liquids with added nanoparticles of Al₂O₃, TiO₂, SiO₂, etc.) are boiling, a significant increase in the critical heat flux is observed [12-16]. For the first time a reasonable explanation for such influence was given by Kim *et al.* [13]. The authors showed that an increase in CHF is primarily caused by the fact that during nanofluid boiling, nanoparticles are deposited on the surface resulting in the formation of a nanocoating. This was confirmed by the results of experiments carried out with pure water boiling on a surface, pre-boiled in a nanofluid, which also

showed an increase in CHF. The formed nanoparticle coatings significantly improve the wetting characteristics; as a result, the heat transfer surfaces become superhydrophilic. However, as it was noted in many papers devoted to nanofluid boiling, including [17, 18], improvement of wettability or decrease in the contact angle is associated not only with changes in the free surface energy of the heat exchange surface, but also with a change in its morphology and porosity, which has also an additional effect on the increase in CHF. The influence of the coatings, formed by nanofluid boiling, on heat transfer remains unclear, and this is caused by contradictory experimental information. For example, in some works, an increase in HTC (heat transfer coefficient) was registered, in others there was heat transfer deterioration; in some works it was shown that the formed coatings have no noticeable effect on heat transfer intensity, but they increase the threshold value for the development of crisis phenomena. The detailed review and analysis of papers dealt with various aspects of nanofluid boiling with a history of development of this problem are presented in [19-21].

The hydrophobic coatings present a certain practical interest in the problems of increasing the efficiency of some heat exchangers, including those for the chemical industry, operating by thermodynamic cycles with coolant boiling. The fact is that the hydrophobic coatings cause a significant reduction in the boiling onset [7, 10-11, 22] with a decrease in the temperature drop of boiling-up and increase in the nucleation site

* To whom all correspondence should be sent:
E-mail: surtaevas@gmail.com

density, and this is important for a number of practical problems. Also, as it is shown in [23], slightly hydrophobic coatings cause fouling inhibition at boiling of water-salt solutions, which is also an actual problem for many types of heat exchangers. However, according to [7, 11], with an increase in hydrophobicity, the heat transfer rate can worsen significantly. Despite the fact that when boiling on a hydrophobic surface, the onset of boiling usually occurs during the first power step, at about 1-2K of wall superheat, the heat transfer data are in qualitative agreement with a film boiling heat transfer trend [7]. Interesting results were obtained by Phan and co-workers [11], where the authors investigated the local and integral characteristics of heat transfer at water boiling ($\Delta T_{sub} \sim 15$ K) on a thin-walled foil (20 μm) by using coatings with different free surface energies and changing contact angle in the range of 22-112°, deposited by using various surface nanomodification techniques, including MOCVD, PECVD and nanofluid boiling. In this work, it is shown that the heat transfer coefficient behaves in a strange way, depending on the contact angle. In particular, in the range $\theta \sim 30$ -90° the heat transfer coefficient decreases as contact angle decreases. At the same time, when the contact angle is varied in the range of $\theta \sim 22$ -31°, improvement of wettability leads to an increase in HTC. The latter trend is also confirmed by the experiments of Takata [9]. In this work, the authors used TiO₂ films as a superhydrophilic coating ($\theta \sim 4$ - 13°). The fact is that under UV irradiation, the TiO₂ films become superhydrophilic for a sufficiently long period. This allows an exclusion of the influence of surface morphology on the boiling process, and investigation of only the influence of wettability. It was found in [9] that the heat transfer coefficient of superhydrophilic TiO₂ increases by 20-30% compared to the surface without coating.

Despite the fact that the wetting properties have a significant effect on the local characteristics of the process and heat transfer intensity at boiling, now there are no reliable theoretical models for describing the observed phenomena. Insufficient understanding of the physics of the process is connected, among other things, with a limited array of experimental information. For example, in [9], the effect of wetting properties in the contact angle range $\theta \sim 0$ -30° on the integral characteristics of the process, namely the heat transfer coefficient and critical heat flux, is analyzed without further theoretical analysis of the experimental results. In more recent works [7, 11], in addition to measuring the heat transfer coefficient, the authors use a high-speed video of the process from the side of the heating surface, which allows them to visualize

evolution of vapor bubbles, measure bubble departure diameter and bubble emission frequency. Nevertheless, this format of recording has several drawbacks, including inability to visualize the dynamics of microlayer and evolution of dry spots under individual vapor bubbles, as well as a high error in determining the nucleation site density, especially in the range of high heat fluxes using hydrophobic coatings.

Recently, the development of modern experimental methods, including high-speed infrared thermography, video recording, laser interferometry, etc., for visualization of the process from the bottom side of a transparent substrate with a thin film heater, allows us to obtain fundamentally new information on nucleation dynamics and heat transfer characteristics at liquid boiling [24-27]. The use of the above spectrum of methods makes it possible to investigate in detail the evolution of vapor bubbles, region and structure of liquid microlayer and dry spots under the different sites, to measure the nucleation site density and frequency of bubble emission over a wide range of heat fluxes, and visualize evolution of the temperature field in various local areas of the surface. Despite the prospects of the above-described high-speed measurement techniques, there are practically no studies in the literature that would allow one to study the effect of nanocoatings with different wetting characteristics on the local and integral characteristics of heat transfer at liquid boiling using these methods. This would make it possible to achieve a significant progress in understanding the fundamental laws governing the influence of wetting properties on the most important parameters characterizing the process of liquid boiling.

In this paper we will present the results of the investigation of the effect of hydrophilic SiO₂ coatings on the internal characteristics of the process (density of nucleation sites, dynamics of vapor bubble growth and departure, evolution of heat under the active nucleation sites, etc.) and heat transfer at water boiling on a transparent heater obtained using modern experimental methods with high temporal and spatial resolution, including video and infrared thermography.

EXPERIMENTAL SETUP

A schematic diagram of the setup for pool boiling experiments is shown in Fig. 1. The detailed description of the experimental facility, heating element and measurement techniques is presented in [27,28]. Deionized water produced by Direct-Q 3 UV water purification system was used as the working liquid. In the experiments 1- μm -thick

films of indium-tin oxide (ITO), vacuum-deposited onto 400- μm -thick sapphire substrates, were used as the heaters. Fabricated samples had an electrical resistance of 2-3 Ohms and a heating area of 20 \times 20 mm². The surface roughness (R_a) of the sapphire substrate was less than 1 nm according to the manufacturer (Hong Yuan Wafer Tech Co). The main advantage of ITO as a heater material in the experiments on investigation of integral and local characteristics of heat transfer at nucleate boiling is its transparency in the visible region (380-750 nm) and opacity in the mid-IR region (3-5 μm) of the spectrum. At the same time, sapphire transmission in the wavelength range of 0.3-5 μm exceeds 80 %. The combination of these properties makes it possible to measure the non-stationary temperature field on the ITO film surface by infrared camera and visually record vapor bubbles dynamics and liquid-vapor system structure directly on the sapphire substrate by high-speed video camera. Therefore, such construction of the heating element was recently widely used for pool boiling experiments [24, 27-29].

Samples were resistively heated (Joule heating) by a DC power supply Elektro Automatik PS 8080-60 DT *via* thin silver electrodes vacuum deposited onto the ITO film. To determine the heat release rate for a given current I , voltage V was measured on the heater with the use of APPA 109N digital multimeter. The heat flux density was calculated as $q = V \cdot I / A$, where A is the area of heater surface. The error in measuring the heat flux density consists of the errors in measuring the voltage in the working section, current and surface area, and does not exceed 3 %.

To visualize the boiling process with high spatial and temporal resolutions, a digital video camera Vision Research Phantom v.7.0 with frame rate up to 20 \cdot 10³ FPS was used. Visualization was performed from the bottom side of the transparent heater, as shown in Fig. 1. To study in detail the evolution of the microlayer and dry spot regions, Nikon 105mm f/2,8G macro lens was used in the work. The maximum spatial resolution of video recording in the experiments was 33 $\mu\text{m}/\text{pix}$. As it will be shown below, this format of visualization allowed us not only to measure the outer diameter of the vapor bubbles, but also to study in detail the evolution of the regions of microlayer and dry spots.

In the experiments the high-speed thermographic camera FLIR Titanium was used to measure the non-stationary temperature field of the heating surface. As configured for this study, the thermographic camera had a frame rate of 1000 FPS and maximum resolution of 150 $\mu\text{m}/\text{pix}$. The total uncertainty of the temperature measurements in the experiments did not exceed 1 K. Due to high thermal conductivity ($k = 25 \text{ W}/\text{m}\cdot\text{K}$) and small thickness of the sapphire substrate, the temperature on its surface was assumed to be equal to the temperature of the ITO film recorded by thermographic camera. The use of IR camera made it possible not only to investigate integral heat transfer at boiling, but also to estimate the nucleation site density, activation temperature and nucleation frequency.

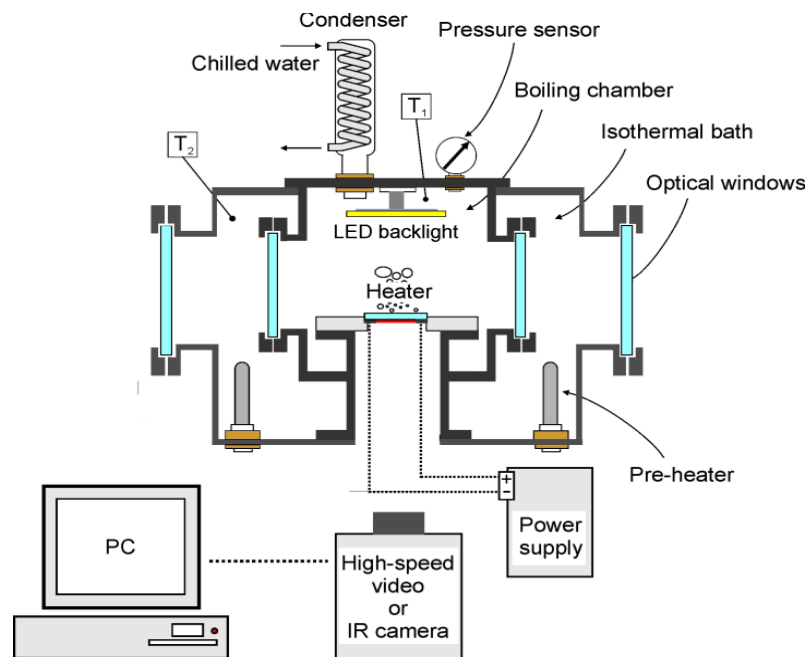


Fig. 1. Scheme of experimental setup.

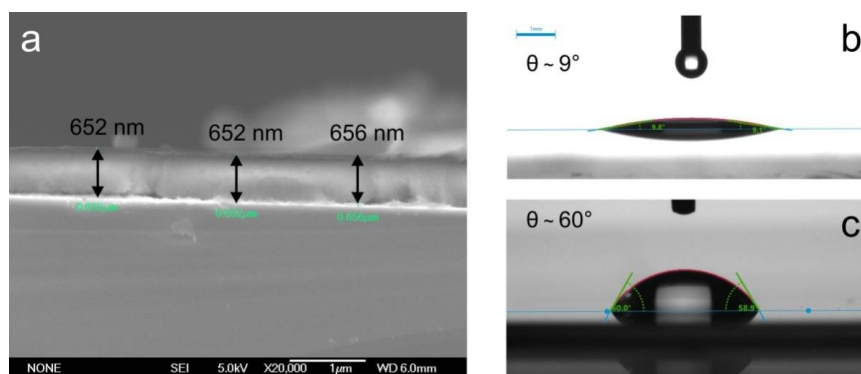


Fig. 2. a – cross-sectional view of the substrate with SiO₂ coating by SEM; b – contact angle measurement with water droplet ($V = 5 \mu\text{l}$) on the SiO₂ coated surface; c – contact angle measurement on the pure sapphire substrate.

Surface modification

The SiO₂ coating was deposited on the sapphire substrate with a view to change the wetting properties of the heat transfer surface *via* dip-coating and spin-coating techniques using a commercial colloidal solution of SiO₂ Ludox AS-30 (30 wt.% SiO₂ in water, pH 9.1), produced by Sigma-Aldrich (USA). After the synthesis, the physico-chemical properties of each sample were analyzed using a complex of modern methods, including nanopprofilometry, electronic spectroscopy and microscopy (EDX, SEM), and KRUSS setup for measuring free surface energy and contact angle. The photograph of a typical SiO₂ coating in cross-sectional view is shown in Fig. 2a. The thickness of the coating was 650 nm. According to the analysis of the water droplet shape on the substrate (Fig. 2b), the SiO₂ coating has hydrophilic properties. Its contact angle reached 9°, which is much less than the value measured on the surface of pure glass and sapphire ($\theta \sim 60^\circ$, Fig. 2c). The analysis of coating morphology also showed that the roughness value R_a does not exceed 3 nm, which is higher than the R_a value for the surface of polished sapphire, but it is significantly smaller than the characteristic value of the critical vapor nucleus for observed superheating of liquid at water boiling.

RESULTS OF EXPERIMENTS

Results of the first series of experiments obtained for the SiO₂ coatings are presented in the paper. To construct boiling curves, experimental data about the heating surface temperature obtained by IR thermography were averaged over the recording time of 10 s and surface area at different heat flux densities. Corresponding boiling curves for water on the heating surfaces with hydrophilic SiO₂ coating and without it are presented in Fig. 3. Analysis of data shows that the coefficients of heat transfer during water boiling on the coated

hydrophilic surface are higher by 20-30% than on the uncoated sapphire surface. This result agrees well with experimental observations of the authors in experiments with water boiling on hydrophilic and superhydrophilic coatings [9, 11].

To determine the possible causes of the influence of SiO₂ coatings on heat transfer, we measured the following local boiling characteristics: growth rate of vapor bubbles, departure diameters, density of nucleation sites (NSD), etc. The latter was measured using synchronized IR thermography and video data. It should be noted that for the analysis of this value by thermograms, the temperature field was averaged over 10 s, and this guaranteed consideration of only constantly active nucleation sites [27]. Analysis shows that the NSD for water boiling on the surface with a hydrophilic coating is lower for the given heat fluxes than that for boiling on the surface of uncoated sapphire (Fig. 4), and this agrees with the theoretical concepts. This result shows that an increase in heat transfer intensity with improvement of wetting properties in the region of low heat fluxes is not associated with an increase in the density of nucleation sites, but it rather is observed on a surface relatively depleted of active sites.

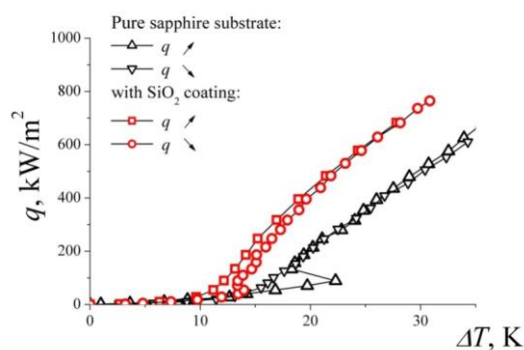


Fig. 3. Boiling curves for saturated water on the pure sapphire surface and surface with SiO₂ coating. The data are presented at both cases – with gradual increase and decrease of heat flux.

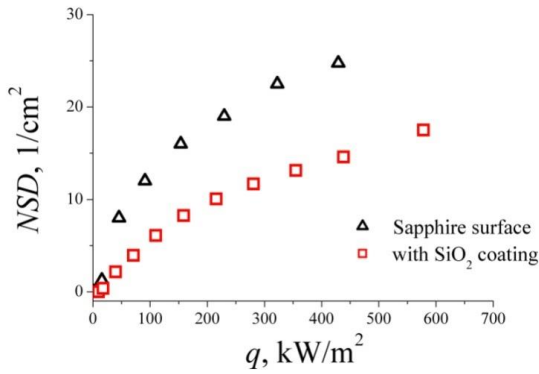


Fig. 4. Dependence of nucleation site density (NSD) on heat flux at water pool boiling on surface with different wettability.

The next step was the analysis of high-speed visualization of the growth dynamics and departure of vapor bubbles, as well as evolution of the microlayer and dry spots under individual bubbles at boiling on a SiO₂ coated surface. Typical video frames of vapor bubble evolution are shown in Fig. 5. In these frames, we can clearly see the outer diameter of the bubble base, microlayer and dry spot regions. In parallel with the analysis, we compared these data with our earlier results obtained for water boiling on a sapphire surface, described in [28, 30]. Histograms of distributions of separated bubble dimensions at boiling on the sapphire substrate and surface with SiO₂ coating at similar heat fluxes are shown in Fig. 6. It can be seen from the figure that the average dimensions of separated bubbles increase noticeably with improvement of the wetting properties. This result

agrees with experimental data of [11]. In that work, water boiling on surfaces with different wetting properties was visualized at the side of the heating surface, which made it impossible to analyze evolution of the microlayer region and dynamics of the contact line at the vapor bubble base. In the present study, such measurements were carried out; in particular, Fig. 7 presents time dependences of the diameter of vapor bubble base, size of microlayer and dry spot region for a single nucleation site. In general, the behavior of curves is similar to the results obtained for water boiling on the surface of pure sapphire without coating. However, as it was noted in [28, 30], when boiling on the sapphire surface, the beginning of bubble departure stage almost coincides with the time of complete liquid evaporation in the microlayer region. The results of measurements on the hydrophilic surface show that for the bubbles with high growth rate and relatively large departure diameter ($D_{dep} > 5$ mm), the stage of separation, when the contact line size decreases (while the outer diameter of the bubble base remains almost constant), begins much earlier than the time of complete evaporation of the liquid microlayer. The measurement results also show that the growth rates of dry spots at water boiling on the hydrophilic surface and surface without coating almost coincide with each other for similar heat fluxes. This suggests that the wetting properties (in the contact angle range $\theta \sim 10 - 60^\circ$) do not affect the dynamics of liquid evaporation in the microlayer region under vapor bubble.

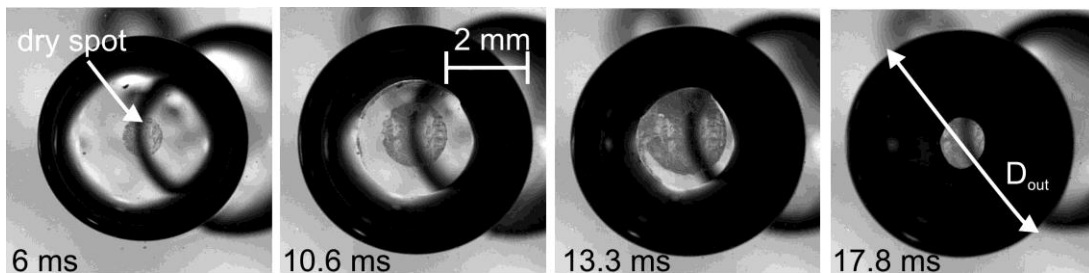


Fig. 5. Frames of high-speed macro visualization of single vapor bubble dynamics at water boiling on the sapphire surface with SiO₂ coating ($q = 26.7$ kW/m²). The time is indicated from the moment of bubble appearance.

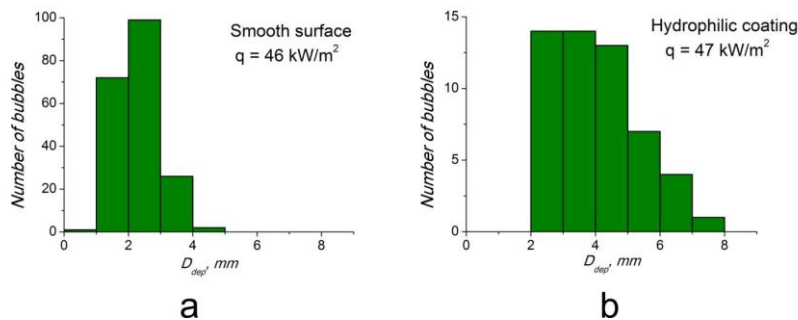


Fig. 6. Effect of surface wettability on the size distribution of separated vapor bubbles obtained at similar heat fluxes.

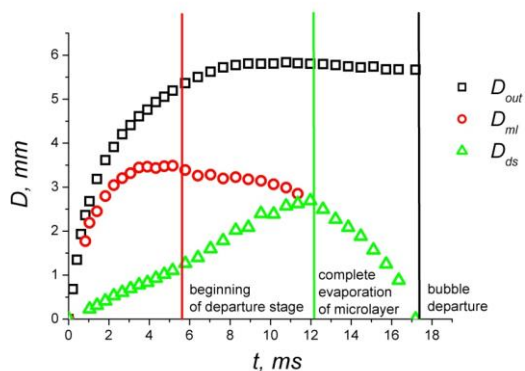


Fig. 7. Evolution of the outer diameter of a single bubble (D_{out}), the region of a microlayer (D_{ml}) and a dry spot (D_{ds}) at water boiling on the sapphire surface with SiO_2 coating ($q = 52.2 \text{ kW/m}^2$).

One of the important local characteristics at boiling is bubble emission frequency. According to the analysis of experimental results on pure sapphire, the value of bubble emission frequency, as well as the value of bubble departure diameter vary in a wide range, for different sites at boiling with a given heat flux. Nevertheless, there is a regularity that bubble emission frequency decreases with an increase in the temperature threshold of site activation and increase in bubble departure diameter. To confirm the above, time dependence of local temperature of the ITO film surface is shown in Fig. 8 for different nucleation sites, where the dimensions of separated bubbles differ significantly, at boiling on the sapphire surface with SiO_2 coating. It can be seen from the figure that the higher the temperature of site activation, the greater is the value of bubble separation diameter and the lower is the bubble emission frequency. On the one hand, it is logical that lower nucleation frequency corresponds to a larger bubble diameter due to an increase in duration of the stage of bubble growth and departure. However, the main contribution to the reduction in nucleation frequency is related to an increase in time of thermal layer restoration and achievement of the threshold temperature of new nucleus activation in the region of low heat fluxes. Thus, it follows that the improvement of the wetting properties not only leads to an increase in bubble departure diameters, but also to a decrease in average nucleation frequency.

The following question arises from the analysis of local boiling characteristics on the sapphire surface with and without SiO_2 coating: what is the main reason for an increase in heat transfer intensity at boiling on a hydrophilic surface? For example, this may be caused by the fact that an increase in bubble departure diameter leads to an increase in the microlayer region and, consequently, to the volume of thin liquid layer

near the heated wall, which means an increase in the heat removed from the heating surface due to intensive evaporation.

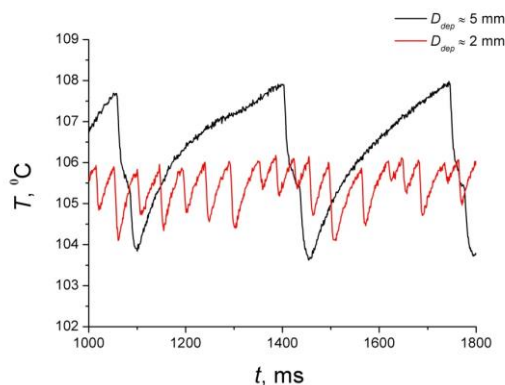


Fig. 8. Dependences of local temperature of the surface with coating on time measured in active nucleation sites with different bubble emission frequency ($q = 52.2 \text{ kW/m}^2$).

In previous works [28, 30], as well as in the present study, it is shown that the size of microlayer region D_{ml} and bubble departure diameter D_{dep} are related by the ratio $D_{ml}/D_{dep} \sim 0.5 - 0.6$ before the beginning of bubble departure stage. In addition, separation of the larger vapor bubbles increases the volume of fresh liquid fed to the heat exchange surface by convection, which increases the amount of heat for thermal layer restoration.

To evaluate the effect of vapor bubbles with different departure diameters, growth rate and activation temperature on heat transfer rate at boiling, we use the mechanistic approach described in [31]. In this approach, it is assumed that the total heat flux removed from the heat exchange surface at liquid boiling is the sum of various components:

$$q_{total} = \frac{q_{ml}t_g + q_r t_w}{t_g + t_w} + q_{nc}, \quad (1)$$

where q_{ml} is heat removed by evaporation of a liquid microlayer at the stage of vapor bubble growth (t_g); q_r is heat required for repeated formation of the destroyed boundary layer at the stage of expectation of bubble appearance after its departure (t_w); q_{nc} is heat transferred by convection on the surface free of bubbles.

To estimate the contribution to heat transfer, we compared two bubbles with significantly different sizes $D_{dep} = 1.2 \text{ mm}$ and $D_{dep} = 5.7 \text{ mm}$ from the data obtained at boiling on a surface with SiO_2 coating ($q = 52.2 \text{ kW/m}^2$). The expressions for q_{ml} and q_r , referred to the unit cycle of a vapor bubble, take the following form:

$$q_{ml} = \rho_l h_{fg} n_f \cdot V_{ml} \quad (2)$$

$$q_r = \frac{2k_l}{\sqrt{\pi\alpha_l t_w}} (na)(T_w - T_{sat}), \quad (3)$$

where f – bubble emission frequency, n – nucleation site density. According to the expression for calculation of q_{ml} , it is necessary to define V_{ml} . In [31], using different approximations, the authors eventually obtain the following expression:

$$q_{ml} = \frac{\gamma\phi\sqrt{\pi}}{10} B^2 Ar^{0.27} Ja(\alpha_l)^{3/2} \sqrt{t_g} \rho_l h_{fg} n, \quad (4)$$

where γ , ϕ , B – empirical constants, Ar – Archimedes number, Ja – Jacob number. In our case, V_{ml} can be calculated directly based on the analysis of data obtained in the present work and data on the liquid microlayer thickness obtained using laser interferometry [26] through simple geometric representation:

$$V_{ml} = \frac{2\pi}{3} \delta_{ml} \frac{D_{dep}^2}{4}. \quad (5)$$

The experimental data on local boiling characteristics required for calculation by (2), (3) and calculation results for q_{ml} and q_r , are given in Table 1 below:

Table 1. Experimental data on local boiling characteristics

D_{dep} , mm	1.2	5.7
ΔT , °C	6	8
f , Hz	27	3.6
t_g , ms	8.8	50
t_w , ms	28.2	226
q_{ml} , kW/m ²	0.28	0.81
q_r , kW/m ²	0.78	7.9

It is seen from the presented results that the ratios q_{ml} and q_r for different nucleation sites are equal to 2.9 and 10, respectively. This suggests that the sites, where the larger vapor bubbles are formed, contribute more to heat transfer at boiling as compared to the sites that generate smaller vapor bubbles with higher nucleation rate. At that, the main contribution to heat transfer is made by the component associated with the non-stationary thermal conductivity and restoration of the thermal boundary layer after vapor bubble departure (q_r) in order to achieve the threshold of site activation temperature. The above estimates also show that the ratio of heat fluxes is so high that despite a decrease in nucleation site density at water boiling on the hydrophilic surface, the heat transfer rate increases in comparison with liquid boiling on a conventional surface.

To verify calculations, the total heat flux q_{total} , delivered to the liquid by all bubbles (1), was

estimated using the experimental data of density of nucleation sites, which showed that the calculated value $q_{total} \approx 48$ kW/m² is in good agreement with the measured value of input heat flux ($q = 52.3$ kW/m²). We should note that in these estimates, we did not take into account the convective component since, as it was shown earlier for pool boiling, q_{ml} and q_r components have the main contribution to q_{total} , and q_{nc} can be neglected [24].

CONCLUSIONS

New fundamental results on the effect of hydrophilic coating on the local and integral characteristics of heat transfer at liquid boiling are obtained in the current research. The use of modern high-speed experimental methods, including IR thermography and video recording, and transparent substrates with a thin film heater and SiO₂ nanocoating, made it possible to determine the following:

- The intensity of heat transfer at water boiling on the surface with hydrophilic SiO₂ coating increases in comparison with boiling on the uncoated sapphire surface, which agrees with the data of [9, 11]. At that, the density of nucleation sites for the given heat fluxes decreases noticeably with improvement of the surface wettability.

- Based on the statistical analysis, it is shown that the dimensions of separated bubbles increase and nucleation frequency decreases at boiling on a hydrophilic surface coated with SiO₂. Based on the visualization analysis, it is shown that a change in the wetting characteristics has no effect on the rate of dry spot growth under vapor bubbles in the region of low heat fluxes.

- Various components of heat transfer at boiling were estimated using the mechanistic approach suggested in [31] and experimental data on local boiling characteristics obtained in the current study for low heat fluxes. It is shown that the increase in quench heat flux q_r (i.e., the transient conduction heat transfer following bubble departure) is the dominant contribution to an increase in nucleate boiling heat transfer on the hydrophilic surface. This fact is associated with an increase in the volume of fresh liquid with increasing size of separated bubbles and increasing temperature threshold of site activation.

Certainly, in order to expand knowledge about influence of surface wettability on local and integral characteristics of the boiling, further investigations with the use of modern high-speed experimental techniques are required in a wide range of wetting properties of the heat exchange surface. According to the authors of this study, transparent photocatalytically active TiO₂

nanocoatings are promising. The fact is that under UV irradiation the surface of TiO₂ coating becomes superhydrophilic with a wetting angle of less than 10°. In addition, the contact angle of TiO₂ can be increased up to 130-140° via subsequent fluorination. Therefore an advantage of TiO₂ coatings for boiling experiments is the possibility to change its wetting properties in a wide range without changing the surface morphology.

Acknowledgement: The reported study was funded by the Russian Foundation for Basic Research according to the research project № 17-08-01342 and Complex Program of Basic Research SB RAS “Interdisciplinary Joint Investigations” (project No. 23, theme AAAA-A18-118022090033-1). We express our gratitude to the Novosibirsk State University for giving us an access to the library.

REFERENCES

1. I. C. Bang, J. H. Jeong, *Nuclear Eng. Technol.*, **43**, 217 (2011).
2. R. Wen, Q. Li, J. Wu, G. Wu, W. Wang, Y. Chen, X. Ma, *Nano Energy*, **33**, 177 (2017).
3. D. Attinger, C. Frankiewicz, A. R. Betz, T. M. Schutzius, R. Ganguly, A. Das, C.-J. Kim, C. M. Megaridis, *MRS Energy Sustainability*, **1**, E4 (2014).
4. C. H. Wang, V. K. Dhir, *J. Heat Transfer*, **115**, 659 (1993).
5. S. G. Kandlikar, *J. Heat Transfer*, **123**, 1071 (2001).
6. M. H. Kim, G. C. Lee, J. Y. Kang, K. Moriyama, H. S. Park, *Int. J. Heat Mass Transfer*, **108**, 1901 (2017).
7. E. Teodori, T. Valente, I. Malavasi, A. S. Moita, M. Marengo, A. L. N. Moreira, *Appl. Therm. Eng.*, **115**, 1424 (2017).
8. H. O'Hanley, C. Coyle, J. Buongiorno, T. McKrell, L. W. Hu, M. Rubner, R. Cohen, *Appl. Phys. Lett.*, **103**, 024102 (2013).
9. Y. Takata, S. Hidaka, J. M. Cao, T. Nakamura, H. Yamamoto, M. Masuda, T. Ito, *Energy*, **30**, 209 (2005).
10. I. I. Gogonin, *Thermophys. Aeromech.*, **17**, 243 (2010).
11. H. T. Phan, N. Caney, P. Marty, S. Colasson, J. Gavillet, *Int. J. Heat Mass Transfer*, **52**, 5459 (2009).
12. S. M. You, J. H. Kim, K. H. Kim, *Appl. Phys. Lett.*, **83**, 3374 (2003).
13. S. J. Kim, I. C. Bang, J. Buongiorno, L. W. Hu, *Int. J. Heat Mass Transfer*, **50**, 4105 (2007).
14. J. S. Coursey, J. Kim, *Int. J. Heat Fluid Flow*, **29**, 1577 (2008).
15. C. Gerardi, J. Buongiorno, L. Hu, T. McKrell, *Nanoscale Res. Lett.*, **1**, 1 (2011).
16. A. R. Neto, J. L. G. Oliveira, J. C. Passos, *Appl. Therm. Eng.*, **111**, 1493 (2017).
17. B. P. Fokin, M. Y. Belenkiy, V. I. Almjashev, V. B. Khabensky, O. V. Almjasheva, V. V. Gusarov, *Tech. Phys. Lett.*, **35**, 440 (2009).
18. H. Kim, E. Kim, M. H. Kim, *Int. J. Heat Mass Transfer*, **69**, 164 (2014).
19. H. Kim, *Nanoscale Res. Lett.*, **6**, 1 (2011).
20. A. S. Surtaev, V. S. Serdyukov, A. N. Pavlenko, *Nanotechnologies in Russia*, **11**, 696 (2016).
21. G. Liang, I. Mudawar, *Int. J. Heat Mass Transfer*, **124**, 423 (2018).
22. B. Bourdon et al., *Int. Commun. Heat Mass Transfer*, **45**, 11 (2013).
23. L. L. Wang, M. Y. Liu, *AIChE J.*, **57**, 1710 (2011).
24. C. Gerardi, J. Buongiorno, L. Hu, T. McKrell, *Int. J. Heat Mass Transfer*, **53**(19), 4185 (2010).
25. I. Golobic, J. Petkovsek, D.B.R. Kenning, *Int. J. Heat Mass Transfer*, **55**, 1385 (2012).
26. S. Jung, H. Kim, *Int. J. Heat Mass Transfer*, **73**, 365 (2014).
27. A. S. Surtaev, V. S. Serdyukov, M. I. Moiseev, *Instrum. Exper. Tech.*, **59**, 615 (2016).
28. A. Surtaev, V. Serdyukov, J. Zhou, A. Pavlenko, V. Tumanov, *Int. J. Heat Mass Transfer*, **126**, 297 (2018).
29. I. C. Chu, H. C. No, C. H. Song, *Int. J. Heat Mass Transfer*, **62**, 142 (2013).
30. A. S. Surtaev, V. S. Serdyukov, *Thermophysics and Aeromechanics*, **25**(1), 67 (2018).
31. R. J. Benjamin, A. R. Balakrishnan, *Int. J. Heat Mass Transfer*, **39**, 2495 (1996).

ХАРАКТЕРИСТИКИ НА ТОПЛОПРЕНАСЯНЕТО ПРИ КИПЕНЕ ВЪРХУ ХИДРОФИЛНА ПОВЪРХНОСТ С ПОКРИТИЕ ОТ SiO₂

А. С. Суртаев^{1,2*}, В.С. Сердюков^{1,2}, А. Н. Павленко¹, Д.В. Козлов^{2,3}, Д.С. Селищев^{2,3}

¹ *Институт по термофизика „Кутателадзе”, Сибирски клон на Руската академия на науките, Новосибирск, 630090, Русия*

² *Новосибирски държавен университет, Новосибирск, 630090, Русия*

³ *Институт по катализ „Боресков”, Сибирски клон на Руската академия на науките, Новосибирск, 630090, Русия*

Постъпила на 17 май, 2018 г.; приета на 26 юни, 2018 г.

(Резюме)

Представени са резултатите от експериментално изследване на влиянието на характеристиките на умокряне върху локалните и интегралните характеристики на топлопреноса при кипене на вода върху линията на насищане при атмосферно налягане. За контрол на характеристиките на умокряне са синтезирани нанопокрития от SiO₂ върху повърхността на сапфирен субстрат чрез различни химични методи, включително покритие чрез потапяне и покритие чрез въртене. С помощта на високоскоростни изобразителни техники като инфрачервена термография и видеи запис на дъното на прозрачен нагревател са получени нови експериментални данни относно динамиката на растеж и откъсване на мехурчета от пара, излъчване на микрослойни и сухи точки, плътност на зародишообразуване, честота на отделяне на мехурчета, топлообмен и др. Чрез анализ на експерименталните данни за локалните и интегралните характеристики на процеса на кипене са установени механизмите на влиянието на хидрофилните покрития върху интензитета на топлопренос.